Inhibition of the CXCL12/CXCR4 axis prevents peri-urethral collagen accumulation and lower urinary tract dysfunction in vivo

Jill A. Macoska, PhD[#1,2], **Zunyi Wang, PhD**[#2,3], **Johanna Virta, BS**[2,3], **Nicholas Zacharias, BS**[2,3], **Dale E. Bjorling, DVM**[2,3]

[1] Center for Personalized Cancer Therapy, The University of Massachusetts Boston, Boston, Massachusetts

[2] Department of Urology, George M. O'Brien Center for Urologic Research, Madison, Wisconsin

[3] School of Veterinary Medicine, The University of Wisconsin Madison, Madison, Wisconsin

[#] These authors contributed equally to this work.

Abstract

Background: Several studies show that prostatic fibrosis is associated with male lower urinary tract dysfunction (LUTD). Development of fibrosis is typically attributed to signaling through the TGFβ pathway, but our laboratory has demonstrated that in vitro treatment of human prostatic fibroblasts with the CXCL12 chemokine stimulates myofibroblast phenoconversion, and that CXCL12 has the capacity to activate profibrotic pathways in these cells in a TGFβ-independent manner. We have previously reported that feeding mice a high fat diet (HFD) results in obesity, II diabetes, increased prostatic fibrosis, and urinary voiding dysfunction. The purpose of this study was to test the hypothesis that in vivo blockade of the CXCL12/CXCR4 axis would inhibit the development of fibrosis-mediated LUTD in HFD fed mice.

Methods: Two month old male SAMP6 mice were fed either a HFD or low fat diet (LFD) for 8 months. Half of each dietary group were given constant access to normal water or water that contained the CXCR4 (CXCL12 receptor) antagonist CXCR4AIII. At the conclusion of the study, mice were weighed, subjected to oral glucose tolerance testing and cystometry, and lower urinary tract tissues collected and assessed for collagen content.

Results: HFD fed mice became significantly obese, insulin resistant, and hyperglycemic, consistent with acquisition of metabolic syndrome, compared to LFD fed mice. Anesthetized cystometry demonstrated that HFD fed mice experienced significantly longer intercontractile intervals and greater functional bladder capacity than LFD fed mice. Immunohistochemistry demonstrated high levels of CXCR4 and CXCR7 staining in mouse prostate epithelial and stromal cells. Picrosirius red staining indicated significantly greater peri-urethral collagen deposition in the prostates of HFD than LFD fedmice. Treatment with the CXCR4 antagonist CXCR4AIII did not

Correspondence Jill A. Macoska, PhD, Center for Personalized Cancer Therapy, Room 4601, Integrated Sciences Complex, 100 Morrissey Blvd The University of Massachusetts, Boston, Boston, MA 02125. Jill.Macoska@umb.edu.

affect acquisition of metabolic syndrome but did reduce both urinary voiding dysfunction and peri-urethral prostate collagen accumulation.

Conclusions: This is the first study to report that obesity-induced lower urinary tract fibrosis and voiding dysfunction can be repressed by antagonizing the activity of the CXCR4 chemokine receptor in vivo. These data suggest that targeting the CXCL12/CXCR4 signaling pathway may be a clinical option for the prevention or treatment of human male lower urinary tract dysfunction.

Keywords

diabetes; mouse; obesity; urinary; voiding

1 | INTRODUCTION

Multiple studies show a clear association between obesity, prostatic inflammation, and clinically significant lower urinary tract symptoms (LUTS). For example, a study of nearly 200 men who were biopsy negative for prostate cancer revealed that elevated central obesity, measured as waist-to-hip ratio (WHR), was significantly associated with moderate/severe LUTS among those participants with prostate tissue inflammation.[1] Reports from the Prostate Cancer Prevention Trial indicated that each 0.05 increase in WHR was associated with a 10% increase of total benign prostatic hyperplasia (BPH) ($P < 0.003$) and severe BPH ($P < 0.02$) as measured by patient-initiated clinical intervention or two or more reports of International Prostate Symptom Score (IPSS) >14 (total) or 20 (severe).[2] A multicenter prospective study that included 378 consecutive men seeking surgical care for enlarged prostate treated with simple open prostatectomy or transurethral resection of the prostate showed that post-treatment LUTS was significantly more severe for men with high (>102 cm) waist circumference.[3] Other studies have demonstrated that morbidly obese bariatric surgery patients reporting urinary voiding dysfunction (stress or urge incontinence) prior to surgery showed significant, rapid, and durable post-operative improvement of their urinary voiding function.[4,5] Taken together, these studies indicate that obesity, particularly central obesity, is associated with LUTS in men.

Several epidemiologic studies suggest that diabetes in men is associated with increased risk for the development of lower urinary tract dysfunction (LUTD), characterized as LUTS, and for increased LUTS severity.[6–9] Diet-induced obesity has also been identified as a risk factor for both type II diabetes mellitus (T2DM) and LUTS in men.[10,11] Conversely, reversion of obesity through weight loss is linked with reduction of symptoms associated with diabetes and LUTS.[12] Interestingly, a study of male diabetic patients found no significant differences in International Prostate Symptom Score (IPSS) or prostate volume between diabetic patients with bladder outlet obstruction (BOO) compared to those without obstructive symptoms. Similarly, a multiethnic community-based study demonstrated positive associations between diabetes and irritative LUTS and nocturia, but not between diabetes across measures more specific to BPH (ie, prostate volume, PSA, and peak urinary flow rate).[13–15] Taken together, these studies found little, if any, association between BOO and diabetes in patients with prostate enlargement, suggesting that the manifestation of LUTS in diabetic men is likely not associated with prostate volume.

A third risk factor for LUTD is inflammation, which is associated with both diabetes and obesity. Immunohistochemical studies examining the histopathology of BPH reported the presence of pervasive inflammatory infiltrate in 90% of specimens obtained from transurethral resection of the prostate (TURP) performed to treat 80 patients diagnosed with BPH/LUTS with no prior history of prostatitis or prostatic infection.[16] Another immunohistochemical study of 282 BPH/LUTS patient specimens found that chronic inflammatory infiltrate was associated with larger prostate volumes and significantly more clinical progression and acute urinary retention.[17] A prospective study of 167 autopsied prostates identified 93 prostate glands harboring BPH, and 75% of these demonstrated inflammatory infiltrate (predominantly chronic inflammation) compared to 50% of those without BPH/LUTS and 55% of those with evidence of cancer[18] The Marberger group previously reported that inflammatory infiltrate was commonly observed in BPH/LUTS specimens and was associated with increased clinical severity and progression.[19–21] More recently, transition zone biopsy specimens from the Medical Therapy of Prostatic Symptoms (MTOPS) trial found that inflammatory infiltrate levels were significantly higher in specimens from men who experienced BPH progression.[22]

Based upon these reports, it is reasonable to postulate that inflammation, perhaps promoted by metabolic syndrome, ie, concurrent obesity and diabetes, is a causative agent in LUTD. In particular, adipokines secreted by obesity-associated white adipose tissue (WAT) are likely central to the development of increased inflammation, impaired extracellular matrix remodeling, and fibrosis observed in multiple organ systems.[23] Mice fed a high fat diet (HFD) develop obesity, insulin resistance, glucosuria, prostatic inflammation, periurethral prostatic fibrosis, and urinary voiding dysfunction, suggesting causal connections between these pathobiologies.[24] Aging prostatic stroma also secretes inflammatory proteins that can attract immune cells, facilitate cellular proliferation, and promote extracellular matrix remodeling.[25–27] In particular, our group has shown that the proinflammatory and pro-fibrotic chemokine, CXCL12, can promote epithelial and stromal fibroblast proliferation, fibroblast to myofibroblast phenoconversion, and collagen accumulation in vitro, and that its cognate receptor, CXCR4, is significantly up-regulated in peri-urethral tissues from men with LUTS.[25,26,28,29] Both white adipose tissue and aging prostate stromal fibroblasts are known to secrete CXCL12.[25,30] However, no studies to-date had specifically tested whether activation of the CXCL12/CXCR4 axis is biologically linked to obesity-induced lower urinary tract fibrosis and voiding dysfunction. We now report that CXCL12/CXCR4 axis blockade represses obesity-induced periurethral collagen accumulation and urinary voiding dysfunction in HFD fed mice. These data suggest that targeting CXCL12/CXCR4 axis activity may be a clinical option to prevent or treat prostatic fibrosis and consequent urinary voiding dysfunction.

2 | MATERIALS AND METHODS

2.1 | Mouse strains and husbandry

The Senescence Accelerated Mouse Prone 6 (SAMP6) mouse strain was used in this study, (Harlan Laboratories, Indianapolis, IN).[31] Senescence-Accelerated Mouse (SAM) models have been developed by selective sister-brother breeding of the AKR/J strain and now

comprise 12 lines: senescence-prone inbred (SAMP) strains 1, 2, 3, 6, 7, 8, 9, 10, and 11, and senescence-resistant (SAMR) strains 1, 4, and 5.[32]The pathobiologies of these mice differ widely, though the SAMP6 strain is characterized by amyloidosis, osteoporosis, and prostatic fibrosis.[32,33] We have previously reported that SAMP6 mice fed a high fat diet develop diet-induced obesity and type II diabetes mellitus concurrent with urinary voiding dysfunction and pronounced prostatic and urethral tissue fibrosis.[24] Mouse husbandry and all procedures were approved by the Institutional Animal Care and Use Committee of the University of Wisconsin-Madison. A breeding colony was established using SAMP6 mice acquired from Harlan Laboratories, Indianapolis, IN.

2.2 | Study design

Male mice were assigned at 8 weeks of age to receive either a low fat diet (LFD; TD 120455; Kcals derived from: protein – 22.3%, carbohydrate – 60.9%, and fat – 16.8%; Envigo Teklad, Madison, WI), or high fat diet (HFD; TD 06414; Kcals derived from: protein – 18.3%, carbohydrates – 21.4%, and fat – 60.3%; Envigo Teklad). Mice were provided fresh chow at least every 3 days and were fed these diets for 8 months. Mice were maintained in a climate and humidity controlled vivarium with a 12 h light/12 h dark cycle and were allowed free access to fresh water. One month after mice began receiving either LFD or HFD, each diet group was further randomly divided to ensure that half the mice in each diet group received regular drinking water and the other half received drinking water containing CXCR4 Antagonist III (CXCR4AIII, product #239822, Millipore Sigma, Burlingham, MA) at a constant concentration of 10 μM for the remainder of the study.[34] Mice were weighed monthly and immediately prior to testing. Testing as subsequently described was performed after mice had received either LFD or HFD for 8 months.

2.3 | Oral glucose tolerance testing and determination of plasma insulin levels

Oral glucose tolerance testing (OGTT) was performed 3–5 days prior to cystometry. Mice were fasted for 5 h prior to OGTT on the day of testing, then received glucose (50%; 2.0 g/kg) by oral gavage. Blood samples were collected from the retro-orbital sinus prior to gavage and 15, 30, 60, and 120 min after gavage. Blood glucose concentrations were measured using a glucometer (AlphaTRAK, Abbott Laboratories, Chicago, IL), and blood samples collected in tubes containing EDTA were placed on ice until centrifuged at 3000 rpm. Plasma samples were stored −80°C for subsequent measurement of insulin. Plasma concentrations of insulin were determined using a commercially available insulin ELISA kit (catalogue number EZMRI-13 K, EMD Millipore, Billerica, MA). Insulin concentrations in all samples were measured at the same time to minimize inter-assay variation.

2.4 | Cystometry

Cystometry was performed in urethane-anesthetized mice as previously described.[35] Mice were weighed, and urethane (1.2 mg/kg) was given subcutaneously. After the mice failed to respond to strong toe pinch (approximately 30 min), an abdominal incision was made through the caudal ventral midline. The bladder was identified, a purse string suture (6–0 silk) was placed in the dome of the bladder, and a cannula (PE 50 tubing) was placed through the purse string and secured with the suture. The abdominal wall and skin were closed with 5–0 suture. Mice were allowed to recover for 1 h, at which time the cannula was

connect to a 3-way stopcock attached to a pressure transducer (Memscap AS, Norway) and infusion pump (Harvard Apparatus, Holliston, MA). Saline (0.9%, 0.8 mL/hr) was infused for 60–90 min to achieve a stable voiding pattern. Bladder pressure was continuously recorded using a PowerLab data collection system (ADInstruments, Colorado Springs, CO) connected to a PC computer. Four to six consecutive micturition recordings were used to determine intercontractile interval (ICI, time between micturitions), maximal micturition pressure (MMP), functional bladder capacity (FBC, determined by multiplying the ICI by the infusion rate), and bladder compliance (volume infused as pressure rose rapidly from baseline to initiation of micturition divided by the change in pressure from baseline to initiation of micturition).

2.5 | Immunohistochemistry

At the conclusion of cystometry, mice were exsanguinated while anesthetized, and tissues were fixed with 10% formalin. The mouse prostate is far more complex than that of humans and is comprised of multiple lobes that extend away from their connection to the urethra. It has previously been observed that the peri-urethral prostatic tissue may more closely resemble that of humans.[36,37] We therefore carefully trimmed the lobes of the prostate away from the prostate tissue immediately adjacent to the urethra under magnification. Tissues were paraffin imbedded, and multiple tissues sections (5 μm) were cut with a microtome. The slides were deparaffinized and rehydrated. For antigen retrieval, slides were incubated in an antigen unmasking solution (H-3300, Vector Laboratories, Burlingame, CA) in boiling water for 30 min. The slides were rinsed, blocked with PBS buffer containing 10 % normal goat serum, 0.1 % BSA and 0.3 % Triton X–100 for 2 h at room temperature, then incubated with primary antibody for 48 h at 4°C, rinsed again, incubated with the corresponding secondary antibody conjugated with biotin for 90 min. The staining was revealed using Elite Vectastin kit and DAB peroxidase substrate solution (both from Vector Laboratories) following manufacturer's instructions. Slides were coverslipped using a xylene based mounting solution from Richard-Allan Scientific (Kalamazoo, MI), examined under Nikon Elipse 600 macroscopy (Nikon Inc., Melville, NY), and images were acquired using Qicam Fast 1394 camera (Qimaging, Surrey, BC, Canada). The primary antibodies used were: rat anti-mouse CXCR4 (1:20, MAB21651, R&D Systems, Minneapolis, MN) and rabbit anti-CXCR7 (1:50, ab72100, Abcam, Cambridge, MA). The secondary antibodies used were: biotinylated goat anti-rat IgG and biotinylated goat anti-rabbit IgG (both used at 1:500, Vector Laboratories). Negative control staining was performed by omitting primary antibody from the procedure. Positive control tissues included breast cancer tissue for CXCR4[38,39] and mouse brain for CXCR7.[40]

2.6 | Tissue processing and collagen assessment

Slides prepared as describe above were examined by viewing sections with bright field microscopy to identify the area of the prostatic urethra where the seminal vesicles and ejaculatory ducts enter the urethra. At least three sections from each prostate cranial to this point were selected for analysis. Slides were stained with picrosirius red (PSR) to identify periurethral abundance of collagen. PSR staining to identify fibrillar collagen was described in 1979[41] and has since become accepted as a sensitive and specific stain for detection of collagen in histological sections.[42,43] PSR is a strong anionic dye that binds to cationic

collagen fibers, enhancing birefringence under polarized light.[41,44] Tissue sections were deparaffinized and rehydrated by incubation with graded concentrations of ethanol, followed by incubation at 25°C for 1 h with PSR (Direct Red 80, 0.5 g, #2610–10-8, Sigma-Aldrich Corp., St. Louis, MO; in 500 mL of saturated picric acid, #P6744–1GA, Sigma-Aldrich Corp). Slides were rinsed with acidified water (0.5% acetic acid), dehydrated with graded ethanol, cleared in xylene, and cover-slipped with Richard-Allan toluene-based mounting medium (#4112APG, Thermo Fisher Scientific, Waltham, MA). Slides were viewed with a Nikon Eclipse E600 microscope (Nikon Instruments Inc., Melville, NY) with and without circular polarized light filters. Images were digitally captured with a Nikon DS-Fi2 camera. Regions of interest for analysis in slides were identified by loading files into Adobe Photoshop (Adobe Systems, San Jose, CA). Tissue adjacent to the urethra routinely showed the most intense PSR staining, and the region of interest of the prostate used for analysis was demarcated ventrally by the urethral sphincter and dorsally by the ejaculatory ducts. The combined area of the lumen of the urethra and lumen of the prostatic ducts within the region of interest was eliminated, and resultant images were analyzed for PSR staining using ImageJ (National Institutes of Health, Bethesda, MD). Background birefringence was corrected prior to analysis to avoid the need for thresholding during analysis. Pixels indicating PSR staining were reported as a percentage of total pixels within the region of interest. Total collagen content of the region of interest was defined as the proportion of positive pixels within birefringent ranges compared to total pixels in the region of interest.

2.7 | Statistical analysis

One-way ANOVA was used to assess differences between groups followed by post-hoc two-sample t-tests to identify statistically significant differences between sub-groups. Arithmetic means and standard errors of the means were calculated for all data sets. Area under the curves was determined for data generated by glucose tolerance testing, and these were compared for effects of diet and treatment. Variance was determined to be equal, and means were compared between treatment groups by two-sample t-test. A value of P 0.05 was considered to indicate significant difference between groups.

3 | RESULTS

3.1 | High fat diet-fed mice develop metabolic syndrome

HFD or HFD + CXCR4 antagonist-fed mice gained significantly ($P < 0.001$) more weight than LFD or LFD + antagonist fed mice (Figure 1). At the conclusion of the study, HFD or HFD + CXCR4 antagonist-fed mice averaged 55.6(+/− 2.9) g or 62(+/− 1.7) g, respectively, compared to LFD or LFD + CXCR4 antagonist-fed mice which averaged 37.1(+/− 1.5) g or 41.4(+/− 3.3) g, respectively, in total body weight. These data show that the HFD promoted obesity that was not affected by the CXCR4 antagonist.

Mice fed a HFD or HFD + CXCR4 also demonstrated significantly higher levels of blood glucose levels, with areas under the curve (AUC) across all time points of 63704(+/2474) mg/dL or 69556 (+/− 2903) mg/dL, respectively, compared to LFD ($P < 0.001$) or LFD + CXCR4 ($P < 0.01$) antagonist-fed mice which averaged 44576 (+/− 3872) mg/dL or 52250(+/− 6596) mg/dL, respectively ($P < 0.001$ and $P < 0.01$, respectively) than those fed

LFD or LFD + CXCR4 antagonist (Figure 2A). This indicates that the HFD diet induced significant hyperglycemia, which was not affected by the CXCR4 antagonist. Lastly, Mice fed a HFD or HFD + CXCR4 demonstrated higher levels of blood insulin levels, with AUCs across all time points averaging 772(+/− 271) ng/mL or 1147(+/− 132) ng/mL, respectively, compared to LFD or LFD + CXCR4 antagonist-fed mice which averaged 385(+/− 37) mg/dL or 573(+/− 69) mg/dL, respectively. Blood insulin values trended higher in HFD and HFD + CXCR4 antagonist-fed mice compared to LFD and LFD + CXCR4 antagonistfed mice. However, these differences did not achieve statistical significance, likely due to the wide range of blood insulin values (263–2535 mg/dL) exhibited by the HFD fed mice (Figure 2B).

Overall, these data indicate that HFD and HFD + CXCR4 antagonist-fed mice developed obesity, hyperglycemia and trended towards developing hyperinsulinemia, consistent with diet-induced metabolic syndrome. These results are largely consistent with previous reports that SAMP6 mice fed a high fat diet develop diet-induced obesity and type II diabetes mellitus, and further indicate that ingestion of the CXCR4 antagonist did not alter this.[24]

3.2 | Peri-urethral mouse prostate tissues express CXCR4

Other studies has shown that CXCR4 and CXCR7 are expressed in the prostates of FVB/N background HiMyc mice.[45] Although CXCL12 primarily signals through CXCR4, its major cognate receptor, it can also bind to CXCR7, another G-protein coupled receptor. CXCR7 is considered an atypical G-protein coupled receptor due to a structural alteration of the N-terminus that disables G_i protein coupling, hence, signal transduction through G_i proteins.[46] We therefore pursued immunohistochemical studies to examine CXCR4 and CXCR7 protein expression levels and localization in SAMP6 mice. As seen in Figure 3, LFD- and HFD-fed mice strongly express CXCR4 and CXCR7, and expression is observed in both epithelial/glandular and stromal compartments. The results of these studies provided rationale to test the effect of blocking CXCR4 activity in LFD- and HFD-fed mice.

3.3 | CXCL12/CXCR4 axis antagonism prevents diet-induced urinary voiding dysfunction

At the end of the study, cystometry was performed to evaluate urinary voiding function by recording 4–6 consecutive micturition recordings to determine intercontractile interval (ICI, time between micturitions), maximal micturition pressure (MMP), functional bladder capacity (FBC, determined by multiplying the ICI by the infusion rate), and bladder compliance (volume infused as pressure rose rapidly from baseline to initiation of voiding divided by the change in pressure from baseline to initiation of voiding). Basal pressure, maximal micturition pressure, and compliance were not significantly altered by diet (Figure 4A). However, interval time between micturitions significantly increased from 484 (+/− 69) s in LFD fed to 723(+/− 54) s in HFD fed mice ($P < 0.05$) (Figure 4B). Similarly, functional bladder capacity increased from 108 (+/− 15) uL in LFD fed to 161(+/− 12) uL in HFD fed mice ($P < 0.05$). However, HFD + CXCR4 antagonist-fed mice did not demonstrate either higher interval times between micturitions or higher bladder capacity compared to LFD or LFD + CXCR4 antagonist-fed mice (Figure 4B). This data shows that HFD negatively alters some aspects of bladder function, and that antagonism of the CXCL12/CXCR4 axis prevents these alterations.

3.4 | CXCL12/CXCR4 axis antagonism reduces diet-induced peri-urethral collagen accumulation

Evaluation of picrosirius red (PSR) stained peri-urethral tissues (Figure 5) showed that the average area of collagen content of these tissues in HFD fed mice, 57(+/− 3.4)%, was significantly ($P< 0.007$) higher than that observed in LFD fed mice, 44(+/− 2.7)% (Figure 6). The average peri-urethral tissue collagen content of LFD + CXCR4 antagonist-fed mice, 48(+/− 2)%, was not significantly different from that of LFD fed mice. However, the average peri-urethral collagen content of HFD + CXCR4 antagonist-fed mice was significantly lower, 41(+/− 2)%, than that of HFD fed mice ($P< 0.004$) and of LFD + CXCR antagonist-fed mice ($P< 0.05$) (Figure 6). These observations indicate that CXCL12/CXCR4 axis activity is coupled to per-urethral collagen accumulation, and that antagonism of this axis reduces collagen deposition in this area within the context of metabolic syndrome. Notably, antagonism of the CXCL12/CXCR4/CXCR7 axis was not associated with changes in CXCR4 or CXCR7 protein expression levels (Figure 3).

4 | DISCUSSION

Metabolic syndrome is a spectrum disorder that can include central obesity, insulin resistance, inflammation, cardiovascular disease, and hyperglycemia.[47]It is increasingly evident that urinary voiding dysfunction in men can be included in this assemblage as a metabolic syndrome-associated co-morbidity.[48,49] Urinary voiding dysfunction is also clearly associated with age and with prior history of prostatic infection/prostatitis.[15,50,51] Therefore, it is challenging to decipher the biological mechanisms associated with metabolic syndrome, aging, and lower urinary tract inflammation that may contribute to the development of urinary voiding dysfunction is challenging.

A common denominator that may link these pathobiologies is the production and secretion of proteins that can act locally as cytokines or differentiation agents on lower urinary tract tissues. White adipose tissue (WAT), which is prevalent in individuals with central obesity and also observed in the HFD fed mouse model used in the current study, is a highly secretory organ known to bathe surrounding tissues in a multitude of pro-proliferative, pro-inflammatory, and pro-fibrotic proteins.[23,24] Prostatic stromal cells, including inflammatory cells and aging prostate fibroblasts, are also highly secretory and can exert similar effects on adjacent tissues.[19–21,25,26] Many of these proteins may act as growth factors to promote prostatic enlargement consistent with benign prostatic hyperplasia (reviewed in Reference Macoska[52]). There is one report in the literature that links high fat diet with prostatic growth and enlargement in a mouse model.[53] This was associated with immune infiltration, basal-to-luminal cellular differentiation in the mouse prostate, and subsequent development of prostatic intraepithelial (PIN)-like lesions that are often antecedent to malignant transformation.[53] Although immune infiltration is observed in concurrent with aging in the SAMP6 mouse model, increased prostatic weight, prostatic growth, or the development of PIN-like lesions is not.[54] Therefore, prostatic enlargement was likely not a factor contributing to the observed urinary voiding dysfunction in the current study.

Consistent with observations from our previous study, prostatic fibrosis, evident as collagen accumulation, was significantly elevated in HFD compared to LFD fed mice.[24] In the

current study, peri-urethral collagen accumulation was associated with urinary voiding dysfunction due to bladder dysfunction, specifically, significantly increased intercontractile interval and functional bladder capacity. Similarly, Gasbarro et al reported increased bladder capacity in diet-induced obese rats and the bladder capacity was further increased in obese rats with type II diabetic conditions.[55] These alterations in bladder function in HFD fed mice could reflect increased urine production associated with type II diabetes. However, treatment with the CXCR4 antagonist neither repressed nor increased HFD-induced hyperglycemia and hyperinsulinemia, but clearly repressed both collagen accumulation and bladder dysfunction. This suggests that the observed increased peri-urethral prostatic fibrosis in HFD fed mice contributed to outflow obstruction, producing the observed significant increases in intercontractile interval and functional bladder capacity. Further studies are required to conclusively link peri-urethral prostatic fibrosis to bladder function.

Perhaps the most significant finding of the current study is that therapeutic disruption of the CXCL12/CXCR4 signaling axis prevented obesity-induced peri-urethral collagen accumulation and bladder dysfunction in vivo. Several studies performed in vitro have shown that activation of the CXCL12/CXCR4 axis induces expression of the COL1A1 and COL1A2 genes and encoded proteins and the phenoconversion of prostate fibroblasts to functional myofibroblasts.[29,56] Studies have also shown that CXCR4 protein levels are elevated in conjunction with high levels of collagen in peri-urethral tissues from men self-reporting moderate/severe LUTS.[28] HFD fed mice exhibit high levels of CXCL12 in both peri-prostatic WAT and prostate ventral lobe stroma, and of CXCR4 and the decoy receptor, CXCR7, in prostate epithelium and stroma in the context of myc-driven prostate tumorigenesis.[45] The current study also demonstrated strong CXCR4 and CXCR7 expression in peri-urethral prostatic epithelium and stroma (Figure 3), and clearly demonstrates that disruption of the CXCL12/CXCR4 axis prevents both peri-urethral collagen accumulation and urinary voiding dysfunction. This finding does not indicate that the CXCL12/CXCR4 axis is the only relevant pro-inflammatory, pro-fibrotic signaling pathway promoting urinary voiding dysfunction in the context of metabolic syndrome. However, it does demonstrate that the CXCL12/CXCR4 axis may be an actionable target for agingand obesity-associated LUTD.

Some limitations of the study should be noted. First, it is not known CXCL12 signals solely through CXCR4, or whether signaling may also occur through CXCR7, in the mouse prostate. The mouse strain used in this study, SAMP6, exhibits strong peri-urethral prostatic CXCR4 and CXCR7 protein expression (Figure 3). Although CXCL12 primarily signals through CXCR4, its major cognate receptor, it can also bind to CXCR7, another G-protein coupled receptor. CXCR7 is considered an atypical G-protein coupled receptor due to a structural alteration of the N-terminus that disables G_i protein coupling, hence, signal transduction through G_i proteins.[46] However, CXCR7 binding to β-arrestin and/or through dimerization with CXCR4 have been postulated as a means for CXCR7-mediated intracellular signal transduction.[57] Our group recently showed that treatment of human prostate stromal fibroblasts with the CXCR4 small molecular inhibitor, AMD3100, completely repressed CXCR4-mediated downstream signaling, collagen expression, and myofibroblast phenoconversion.[29] Although the small molecular inhibitor used in the current study, CXCR4AIII, interacts with CXCR4 with high specificity, it is not known whether it

also interacts with CXCR7.[34] Given the significant decrease in HFD-mediated collagen accumulation and urinary voiding dysfunction observed in mice treated with CXCR4AIII, however, it is likely that CXCR4 is the major signaling receptor of the CXCL12/CXCR4/CXCR7 axis in the mouse prostate. Second, the number of mice examined in the study was relatively small. Although the study aimed to include 12 mice/group, the low fat diet in particular was not well tolerated by the mice which reduced the final number of mice in the low fat diet control and treatment groups. However, the data shows a clear distinction between HFD and LFD fed mice, suggesting that the major results and conclusions would not have changed significantly by including a higher number of mice in the study. Third, the current study is somewhat "prostate centric," although metabolic syndrome impacts multiple organ systems and physiological processes. A recent study by Denys et al suggested that metabolic syndrome is minimally associated with sleep disorders, renal dysfunction, and bladder dysfunction, all of which can contribute to LUTD.[48] Therefore, perhaps a more systematic evaluation of these parameters in diet-induced mouse obesity models could elucidate the full impact of metabolic disorder on urinary voiding dysfunction.

5 | CONCLUSIONS

This is the first study to report that obesity-induced lower urinary tract fibrosis and voiding dysfunction can be repressed by therapeutically antagonizing the activity of the CXCR4 chemokine receptor in vivo. Specifically, the development of peri-urethral collagen accumulation and bladder dysfunction was blocked through the systemic administration of a water-soluble small molecular inhibitor of CXCL12. These data suggest that targeting the CXCL12/CXCR4 signaling pathway may be a clinical option for prevention or treatment of human male lower urinary tract dysfunction.

ACKNOWLEDGMENTS

REFERENCES

1. Fowke JH, Koyama T, Fadare O, Clark PE. Does inflammation mediate the obesity and BPH relationship? an epidemiologic analysis of body composition and inflammatory markers in blood, urine, and prostate tissue, and the relationship with prostate enlargement and lower urinary tract symptoms. PLoS ONE. 2016; 11:e0156918. [PubMed: 27336586]

2. Kristal AR, Arnold KB, Schenk JM, et al. Race/ethnicity, obesity, health related behaviors and the risk of symptomatic benign prostatic hyperplasia: results from the prostate cancer prevention trial. J Urol. 2007;177: 1395–1400. [PubMed: 17382740]

3. Gacci M, Sebastianelli A, Salvi M, et al. Central obesity is predictive of persistent storage lower urinary tract symptoms (LUTS) after surgery for benign prostatic enlargement: results of a multicentre prospective study. BJU Int. 2015;116: 271–277. [PubMed: 25597623]

4. Aleid M, Muneer A, Renshaw S, et al. Early effect of bariatric surgery on urogenital function in morbidly obese men. J Sex Med. 2017;14: 205–214. [PubMed: 28087357]

5. Subak LL, King WC, Belle SH, et al. Urinary incontinence before and after bariatric surgery. JAMA Intern Med. 2015;175: 1378–1387. [PubMed: 26098620]

6. Klein BE, Klein R, Lee KE, Bruskewitz RC. Correlates of urinary symptom scores in men. Am J Public Health. 1999;89: 1745–1748. [PubMed: 10553401]

7. Joseph MA, Harlow SD, Wei JT, et al. Risk factors for lower urinary tract symptoms in a population-based sample of African-American men. Am J Epidemiol. 2003;157:906–914. [PubMed: 12746243]

8. Michel MC, Mehlburger L, Schumacher H, Bressel HU, Goepel M. Effect of diabetes on lower urinary tract symptoms in patients with benign prostatic hyperplasia. J Urol. 2000;163: 1725–1729. [PubMed: 10799169]

9. Koskimaki J, Hakama M, Huhtala H, Tammela TL. Association of nonurological diseases with lower urinary tract symptoms. Scand J Urol Nephrol. 2001;35: 377–381. [PubMed: 11771864]

10. Parsons JK. Benign prostatic hyperplasia and male lower urinary tract symptoms: epidemiology and risk factors. Curr Bladder Dysfunct Rep. 2010;5: 212–218. [PubMed: 21475707]

11. Parsons JK, Sarma AV, McVary K. Wei JT. Obesity and benign prostatic hyperplasia: clinical connections, emerging etiological paradigms and future directions. J Urol. 2013;189:S102–S106. [PubMed: 23234610]

12. Khoo J, Piantadosi C, Duncan R, et al. Comparing effects of a low-energy diet and a high-protein low-fat diet on sexual and endothelial function, urinary tract symptoms, and inflammation in obese diabetic men. J Sex Med. 2011;8: 2868–2875. [PubMed: 21819545]

13. Meigs JB, Mohr B, Barry MJ, Collins MM, McKinlay JB. Risk factors for clinical benign prostatic hyperplasia in a community-based population of healthy aging men. J Clin Epidemiol. 2001;54: 935–944. [PubMed: 11520654]

14. Verhamme KM, Dieleman JP, Bleumink GS, et al. Incidence and prevalence of lower urinary tract symptoms suggestive of benign prostatic hyperplasia in primary care?the Triumph project. European Urol. 2002;42:323–328.

15. Guess HA. Benign prostatic hyperplasia: antecedents and natural history. Epidemiol Rev. 1992;14:131–153. [PubMed: 1283852]

16. Nickel JC, Downey J, Young I, Boag S. Asymptomatic inflammation and/or infection in benign prostatic hyperplasia. BJU Int. 1999;84: 976–981. [PubMed: 10571623]

17. Robert G, Descazeaud A, Nicolaïew N, et al. Inflammation in benign prostatic hyperplasia: a 282 patients' immunohistochemical analysis. Prostate. 2009;69: 1774–1780. [PubMed: 19670242]

18. Delongchamps NB, de la Roza G, Chandan V, et al. Evaluation of prostatitis in autopsied prostates–is chronic inflammation more associated with benign prostatic hyperplasia or cancer? J Urolo. 2008;179:1736–1740.

19. Theyer G, Kramer G, Assmann I, et al. Phenotypic characterization of infiltrating leukocytes in benign prostatic hyperplasia. Lab Invest. 1992;66: 96–107. [PubMed: 1370561]

20. Steiner GE, Stix U, Handisurya A, et al. Cytokine expression pattern in benign prostatic hyperplasia infiltrating T cells and impact of lymphocytic infiltration on cytokine mRNA profile in prostatic tissue. Lab Invest. 2003;83: 1131–1146. [PubMed: 12920242]

21. Kramer G, Mitteregger D, Marberger M. Is benign prostatic hyperplasia (BPH) an immune inflammatory disease? Eur Urol. 2007;51: 1202–1216. [PubMed: 17182170]

22. Torkko KC, Wilson RS, Smith EE, Kusek JW, van Bokhoven A, Lucia MS. Prostate biopsy markers of inflammation are associated with risk of clinical progression of benign prostatic hyperplasia: findings from the MTOPS study. J Urol. 2015;194: 454–461. [PubMed: 25828974]

23. Unamuno X, Gomez-Ambrosi J, Rodriguez A, Becerril S, Fruhbeck G, Catalan V. Adipokine dysregulation and adipose tissue inflammation in human obesity. Eur J Clin Invest. 2018;48: e12997. [PubMed: 29995306]

24. Gharaee-Kermani M, Rodriguez-Nieves JA, Mehra R, Vezina CA, Sarma AV, Macoska JA. Obesity-induced diabetes and lower urinary tract fibrosis promote urinary voiding dysfunction in a mouse model. Prostate. 2013;73:1123–1133. [PubMed: 23532836]

25. Begley L, Monteleon C, Shah RB, Macdonald JW, Macoska JA. CXCL12 overexpression and secretion by aging fibroblasts enhance human prostate epithelial proliferation in vitro. Aging Cell. 2005;4: 291–298. [PubMed: 16300481]

26. Begley LA, Kasina S, MacDonald J, Macoska JA. The inflammatory microenvironment of the aging prostate facilitates cellular proliferation and hypertrophy. Cytokine. 2008;43: 194–199. [PubMed: 18572414]

27. McDowell KL, Begley LA, Mor-Vaknin N, Markovitz DM, Macoska JA. Leukocytic promotion of prostate cellular proliferation. Prostate. 2010;70: 377–389. [PubMed: 19866464]

28. Gharaee-Kermani M, Kasina S, Moore BB, Thomas D, Mehra R. Macoska JA. CXC-Type chemokines promote myofibroblast phenoconversion and prostatic fibrosis. PLoS ONE. 2012;7: e49278. [PubMed: 23173053]

29. Rodriguez-Nieves JA, Patalano SC, Almanza D, Gharaee-Kermani M, Macoska JA. CXCL12/CXCR4 axis activation mediates prostate myofibroblast phenoconversion through non-Canonical EGFR/MEK/ERK signaling. PLoS ONE. 2016;11: 0159490.

30. Kim D, Kim J, Yoon JH, et al. CXCL12 secreted from adipose tissue recruits macrophages and induces insulin resistance in mice. Diabetologia. 2014;57: 1456–1465. [PubMed: 24744121]

31. Takeda T, Hosokawa M, Higuchi K. Senescence-accelerated mouse (SAM): a novel murine model of senescence. Exp Gerontol. 1997;32:105–109. [PubMed: 9088907]

32. Takeda T, Matsushita T, Kurozumi M, Takemura K, Higuchi K, Hosokawa M. Pathobiology of the senescence-accelerated mouse (SAM). Exp Gerontol. 1997;32:117–127. [PubMed: 9088909]

33. Azuma K, Zhou Q, Kubo KY. Morphological and molecular characterization of the senile osteoporosis in senescence-accelerated mouse prone 6 (SAMP6). Med Mol Morphol. 2018;51: 139–146. [PubMed: 29619545]

34. Wu CH, Chang CP, Song JS, et al. Discovery of novel stem cell mobilizers that target the CXCR4 receptor. ChemMedChem. 2012;7: 209–212. [PubMed: 22190478]

35. Bjorling DE, Wang Z, Vezina CM, et al. Evaluation of voiding assays in mice: impact of genetic strains and sex. Am J Physiol Renal Physiol. 2015;308: F1369–F1378. [PubMed: 25904700]

36. Nicholson TM, Ricke EA, Marker PC, et al. Testosterone and 17beta-estradiol induce glandular prostatic growth, bladder outlet obstruction, and voiding dysfunction in male mice. Endocrinology. 2012;153: 5556–5565. [PubMed: 22948219]

37. Nicholson TM, Ricke WA. Androgens and estrogens in benign prostatic hyperplasia: past, present and future. Differentiation. 2011;82:184–199. [PubMed: 21620560]

38. Del Molino Del Barrio I, Wilkins GC, Meeson A, Ali S, Kirby JA. Breast cancer: an examination of the potential of ACKR3 to modify the response of CXCR4 to CXCL12. Int J Mol Sci. 2018;19.

39. Luker KE, Lewin SA, Mihalko LA, et al. Scavenging of CXCL12 by CXCR7 promotes tumor growth and metastasis of CXCR4-positive breast cancer cells. Oncogene. 2012;31: 4750–4758. [PubMed: 22266857]

40. Banisadr G, Podojil JR, Miller SD, Miller RJ. Pattern of CXCR7 gene expression in mouse brain under normal and inflammatory conditions. J Neuroimmune Pharmacol. 2016;11: 26–35. [PubMed: 25997895]

41. Junqueira LC, Bignolas G, Brentani RR. Picrosirius staining plus polarization microscopy, a specific method for collagen detection in tissue sections. Histochem J. 1979;11: 447–455. [PubMed: 91593]

42. Lattouf R, Younes R, Lutomski D, et al. Picrosirius red staining: a useful tool to appraise collagen networks in normal and pathological tissues. J Histochem Cytochem. 2014;62: 751–758. [PubMed: 25023614]

43. Wegner KA, Keikhosravi A, Eliceiri KW, Vezina CM. Fluorescence of picrosirius red multiplexed with immunohistochemistry for the quantitative assessment of collagen in tissue sections. J Histochem Cytochem. 2017;65: 479–490. [PubMed: 28692327]

44. Montes GS, Junqueira LC. The use of the Picrosirius-polarization method for the study of the biopathology of collagen. Memorias do Instituto Oswaldo Cruz. 1991;86:1–11.

45. Saha A, Ahn S, Blando J, Su F, Kolonin MG, DiGiovanni J. Proinflammatory CXCL12-CXCR4/CXCR7 signaling axis drives myc-Induced prostate cancer in obese mice. Cancer Res. 2017;77:5158–5168. [PubMed: 28687617]

46. Graham GJ, Locati M, Mantovani A, Rot A, Thelen M. The biochemistry and biology of the atypical chemokine receptors. Immunol Lett. 2012;145:30–38. [PubMed: 22698181]

47. Eckel RH, Grundy SM, Zimmet PZ. The metabolic syndrome. Lancet. 2005;365: 1415–1428. [PubMed: 15836891]

48. Denys MA, Anding R, Tubaro A, Abrams P, Everaert K. Lower urinary tract symptoms and metabolic disorders: iCI-RS 2014. Neurourol Urodyn. 2016;35: 278–282. [PubMed: 26872568]

49. Pashootan P, Ploussard G, Cocaul A, de Gouvello A, Desgrandchamps F. Association between metabolic syndrome and severity of lower urinary tract symptoms (LUTS): an observational study in a 4666 European men cohort. BJU Int. 2015;116: 124–130. [PubMed: 25229124]

50. Collins MM, Stafford RS, O'Leary MP, Barry MJ. Distinguishing chronic prostatitis and benign prostatic hyperplasia symptoms: results of a national survey of physician visits. Urology. 1999;53: 921–925. [PubMed: 10223484]

51. Collins MM, Meigs JB, Barry MJ, Walker Corkery E, Giovannucci E, Kawachi I. Prevalence and correlates of prostatitis in the health professionals follow-up study cohort. J Urol. 2002;167: 1363–1366. [PubMed: 11832733]

52. Macoska JA. Chemokines and BPH/LUTS. Differentiation. 2011;82: 253–260. [PubMed: 21600689]

53. Kwon OJ, Zhang B, Zhang L, Xin L. High fat diet promotes prostatic basal-to-luminal differentiation and accelerates initiation of prostate epithelial hyperplasia originated from basal cells. Stem Cell Res. 2016;16: 682–691. [PubMed: 27107344]

54. Sugimura Y, Sakurai M, Hayashi N, Yamashita A, Kawamura J. Age-related changes of the prostate gland in the senescence-accelerated mouse. Prostate. 1994;24: 24–32. [PubMed: 7507239]

55. Gasbarro G, Lin DL, Vurbic D, et al. Voiding function in obese and type 2 diabetic female rats. Am J Physiol Renal Physiol. 2010;298: F72–F77. [PubMed: 19889955]

56. Gharaee-Kermani M, Moore BB, Macoska JA. Resveratrol-Mediated repression and reversion of prostatic myofibroblast phenoconversion. PLoS ONE. 2016;11: e0158357. [PubMed: 27367854]

57. Pawig L, Klasen C, Weber C, Bernhagen J, Noels H. Diversity and inter-Connections in the CXCR4 chemokine Receptor/Ligand family: molecular perspectives. Front Immunol. 2015;6:429. [PubMed: 26347749]
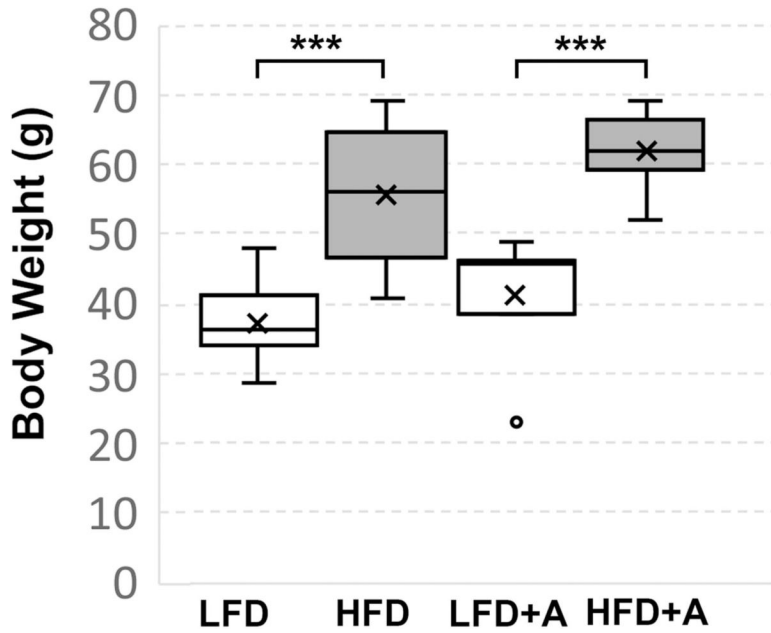
FIGURE 1.

High fat diet-fed mice develop obesity. Box and whisker plots of total body weight of HFD
($N=11$), HFD + CXCR4 antagonist (HFDA) ($N=9$), LFD ($N=7$), or LFD + CXCR4
antagonist (LFDA) ($N=12$) fed mice. HFD or HFD + CXCR4 antagonist-fed mice averaged
55.6(+/− 2.9) g or 62(+/− 1.7) g, respectively, compared to LFD or LFD + CXCR4
antagonist-fed mice, which averaged 37.1 (+/− 1.5) g or 41.4(+/− 3.3) g in total body weight.
HFD or HFDA fed mice gained significantly ($P < .001$) more weight than LFD or LFDA fed
mice. Treatment with the CXCR4 antagonist did not affect weight gain in any group. Box
plots indicate lower extreme, lower quartile, median (line), mean (x), upper quartile and
upper extreme. Statistical significance between groups is indicated as *, $P < 0.01$; **, $P < 0.001$; ***, $P > 0001$
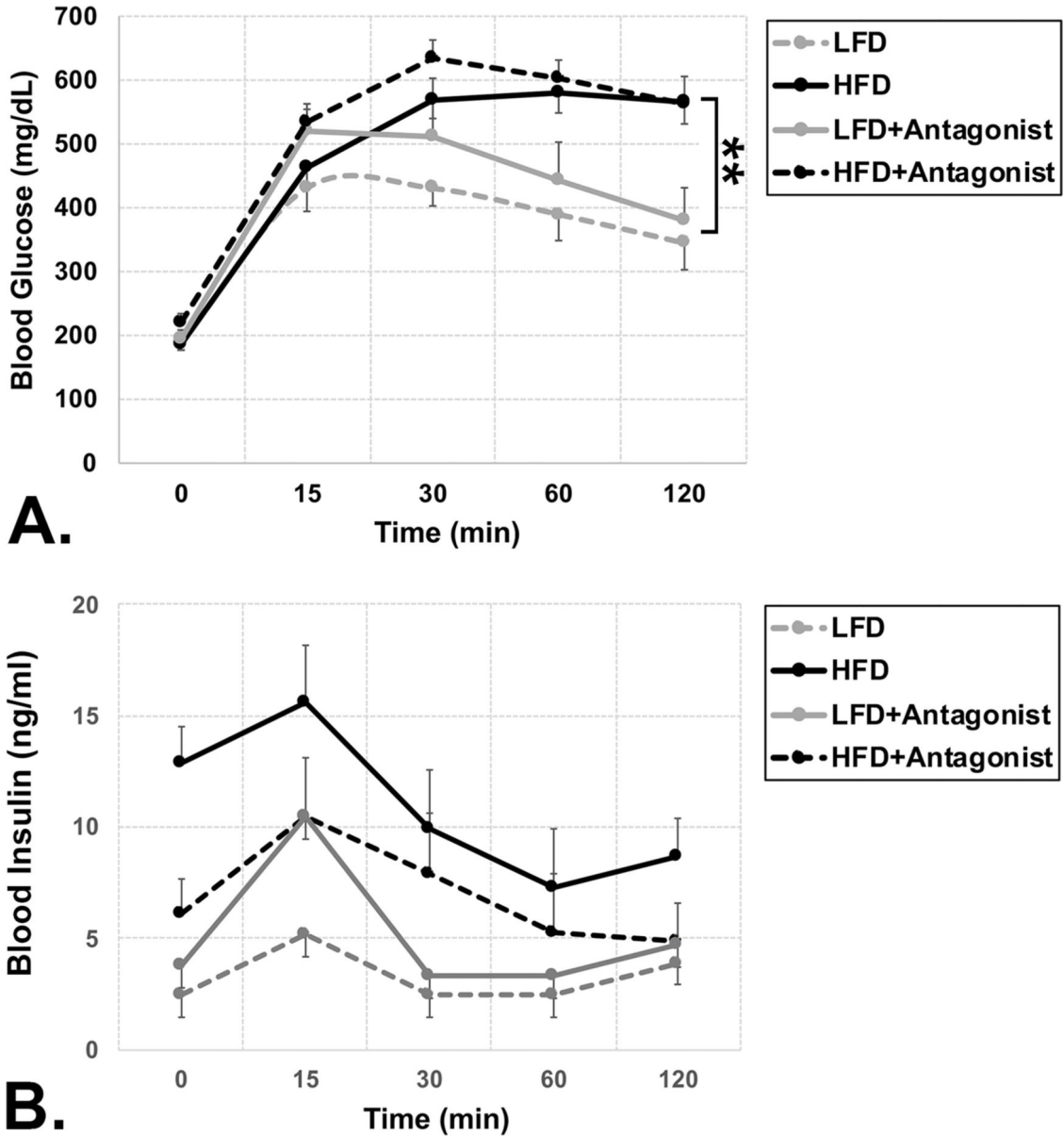
FIGURE 2.

High fat diet-fed mice develop diabetes. A) Plot of oral glucose tolerance test (OGTT) results showing blood glucose levels at 0, 15, 30, 60, and 120 min following 5 h fast and oral gavage of glucose bolus (50%; 2.0 g/kg). Mice fed a HFD ($N = 11$) or HFD + CXCR4 antagonist (HFDA) ($N = 9$) diet demonstrated significantly higher levels of blood glucose levels, with areas under the curve (AUC) across all time points of 63704(+/2474) mg/dL or 69556(+/− 2903) mg/dL, respectively, compared to mice fed a LFD ($N = 7$) or LFD + CXCR4 antagonist (LFDA) ($N = 12$) diet, which averaged 44576(+/− 3872) mg/dL or 52250(+/− 6596) mg/dL, respectively. This indicates that the HFD diet induced significant hyperglycemia, which was not affected by the CXCR4 antagonist. B) Plot of oral glucose tolerance test (OGTT) results showing blood insulin levels at 0, 15, 30, 60, and 120 min following 5 h fast and oral gavage of glucose bolus (50%; 2.0 g/kg). Mice fed a HFD ($N=$

11) or HFD + CXCR4 antagonist (HFDA) ($N = 9$) diet demonstrated higher levels of blood insulin levels, with AUCs across all time points averaging 772(+/− 271) ng/mL or 1147(+/− 132) ng/mL, respectively, mice fed a LFD ($N = 7$) or LFD + CXCR4 antagonist (LFDA) ($N = 12$) diet, which averaged 385(+/− 37) mg/dL or 573(+/− 69) mg/dL, respectively. Blood insulin values trended higher in HFD and HFD + CXCR4 antagonist-fed mice compared to LFD and LFD + CXCR4 antagonist-fed mice. However, these differences did not achieve statistical significance. Statistical significance between groups is indicated as *, $P < 0.01$; **, $P < 0.001$; ***, $P > 0001$
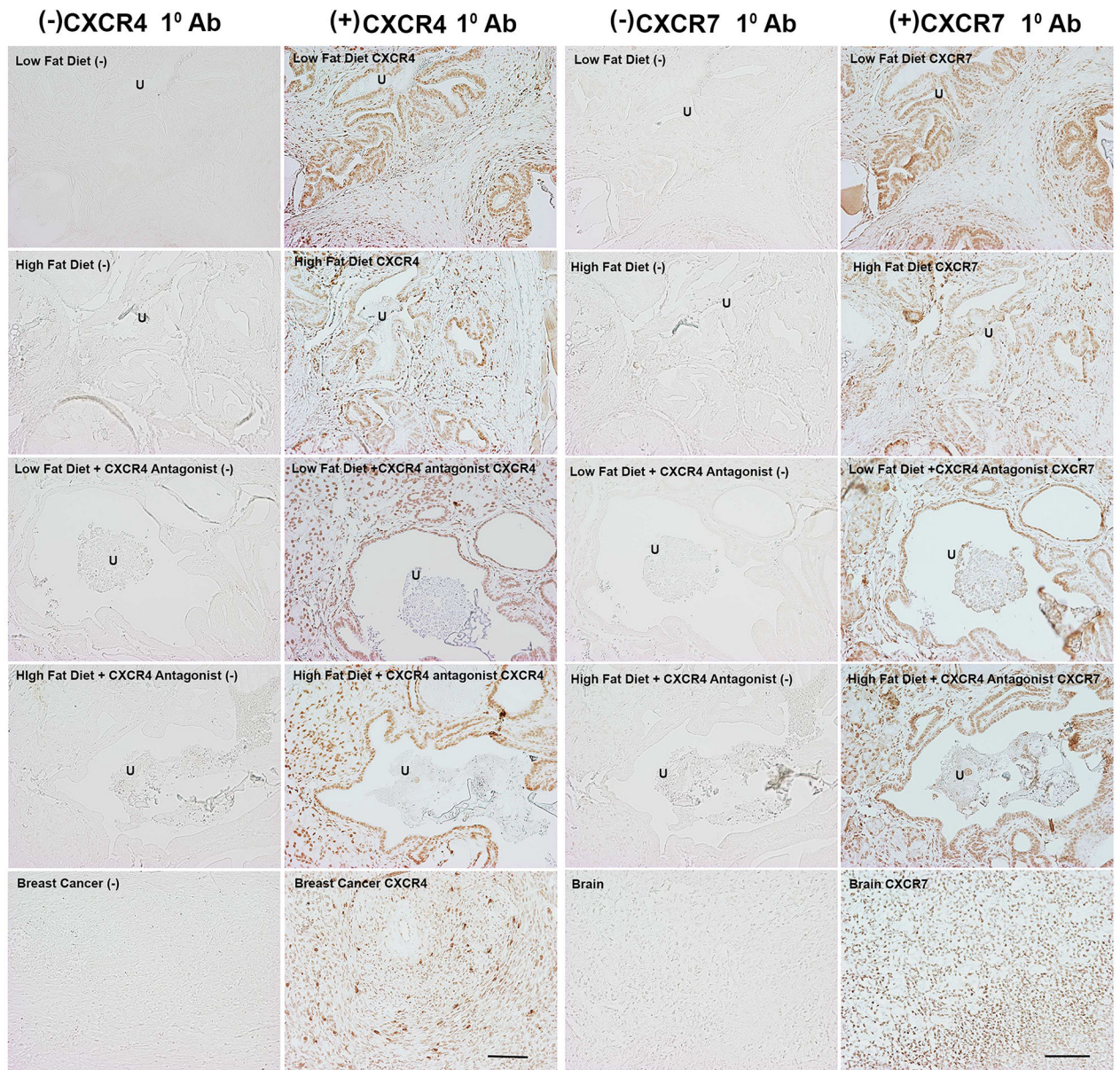
FIGURE 3.

Immunohistochemical staining of CXCR4 and CXCR7 in prostatic urethral tissues from LFD- and HFD-fed mice. Representative bright field images of prostatic urethral tissues stained for CXCR4 (left) or CXCR7 (right) protein expression from LFD- or HFD-fed mice. Photomicrographs show tissues stained with anti-rat secondary antibody [indicated as Low Fat Diet or High Fat Diet], with both rat anti-mouse primary CXCR4 and anti-rat secondary antibodies [indicated as Low Fat Diet CXCR4 or High Fat Diet CXCR4] fed regular drinking water (indicated as +CXCR4 Antagonist [−]), or fed drinking water containing CXCR4 Antagonist III (indicated as +CXCR4 Antagonist CXCR4). Similar nomenclature is used for the right panels except that the antibodies used were goat anti-rabbit secondary antibody or rabbit anti-mouse primary CXCR7 antibody. Human breast cancer and mouse brain were stained with secondary alone or primary + secondary antibodies as indicated.

Tissues stained with primary CXCR4 or CXCR7 antibodies demonstrate expression of both receptors in both glandular and stromal areas. Treatment with the CXCR4 Antagonist did not increase or diminish expression of CXCR4 or CXCR7. U, urethra. Scale bar = 100 μm. [Color figure can be viewed at wileyonlinelibrary.com]

| Parameter (units)	Diet and Treatment					p-value
	LFD	HFD	LFD + Antagonist	HFD + Antagonist		
Basal Pressure (mmHg)	4.6	3.9	3.7	3.8	Mean	0.34846
	0.6	0.3	0.4	0.2	SEM	
Maximal Micturition Pressure (mmHg)	19.2	20.3	22.8	20.8	Mean	0.52127
	2.2	2	1.4	1.7	SEM	
Interval Time between Micturitions (s)	484.2*	722.6*	515.6	642.6	Mean	**0.03318**
	68.9	53.5	80	53.3	SEM	
Functional Bladder Capacity (ul)	107.6*	160.6*	114.6	142.8	Mean	**0.03318**
	15.3	11.9	17.8	11.8	SEM	
Voiding Duration (s)	3.9	4.3	4.4	4.2	Mean	0.81424
	0.3	0.2	0.6	0.3	SEM	
Compliance (ml/mmHg)	0.018	0.022	0.028	0.025	Mean	0.61539
	0.004	0.002	0.009	0.004	SEM	

**A.**
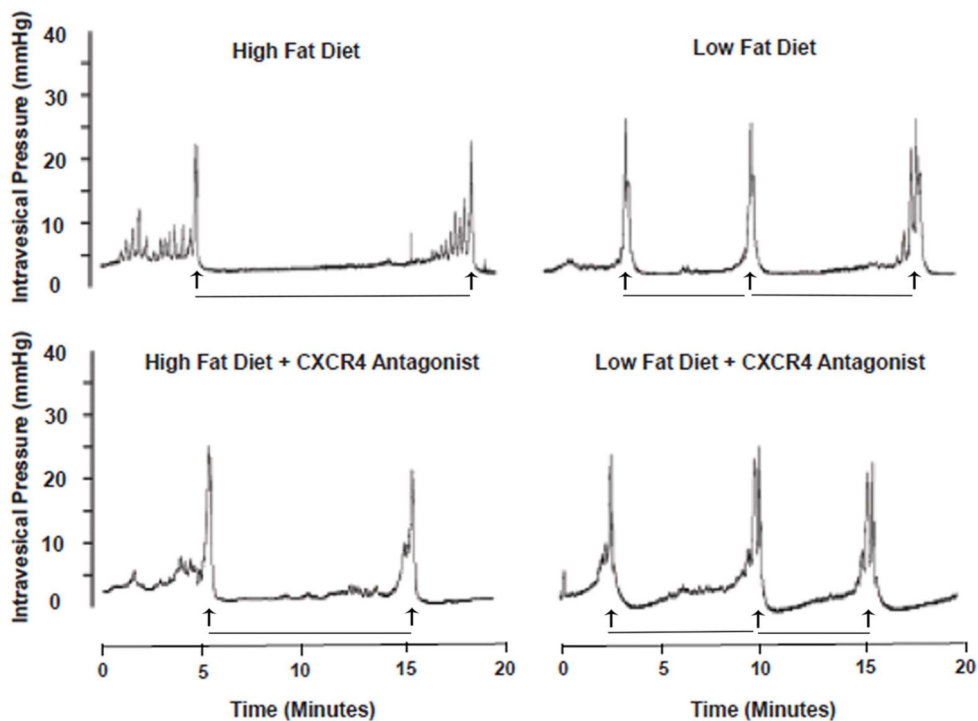
B.

FIGURE 4.

Cystometric Measurement of Urinary Voiding Function. A) Cystometry was performed in urethane-anesthetized mice as previously described.[35] Bladder pressure was continuously recorded using a PowerLab data collection system connected to a PC computer. Four to six consecutive micturition recordings were used to determine intercontractile interval (ICI, time between micturitions), maximal micturition pressure (MMP), functional bladder capacity (FBC, determined by multiplying the ICI by the infusion rate), and bladder compliance (volume infused as pressure rose rapidly from baseline to initiation of voiding divided by the change in pressure from baseline to initiation of voiding). HFD fed mice demonstrated significantly higher interval time between micturitions ($P = 0.033$) and functional bladder capacity ($P = 0.033$) compared to all other groups. HFD + CXCR4 antagonist, LFD, and

LFD + CXCR4 antagonist-fed mice did not demonstrate any measures of urinary voiding dysfunction. B) Cystometrogram plots (CMG) of intravesical pressure (mmHg) versus time (min). The interval time between micturitions (indicated as minutes between vertical arrows) significantly increased from 484(+/− 69) s in LFD fed to 723(+/− 54) s in HFD fed mice ($P < 0.05$). HFD + CXCR4 antagonist fed mice did not demonstrate higher interval times between micturitions compared to LFD or LFD + CXCR4 antagonist fed mice
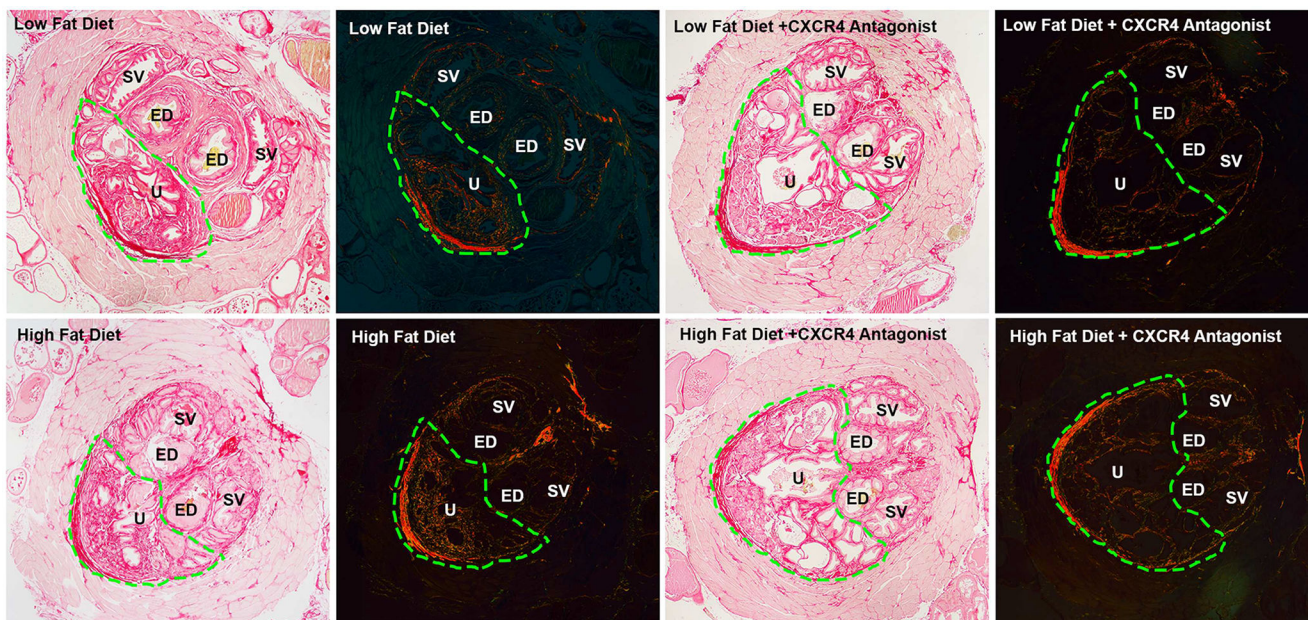
FIGURE 5.

Picrosirius red stained sections of peri-urethral prostate tissues. Representative bright field images for each group are on the left and the same section viewed with polarized light is on the right. The region of interest is outlined by the green dotted line which includes urethra (U) and prostatic tissue ventral to the ejaculatory ducts (ED). The area of the urethra and prostatic ducts within the region of interest was excluded from determination of total area, and the number of pixels present was normalized to the remaining area within the region of interest. Increased collagen fibers were present within the region of interest in HFD fed mice, and this was decreased in HFD fed mice that received the CXCR4 antagonist. The light pink tissue surrounding the peri-urethral prostate is the rhabdosphincter. U, urethra; ED, ejaculatory duct; SV, seminal vesicle. All images at 40×. [Color figure can be viewed at wileyonlinelibrary.com]
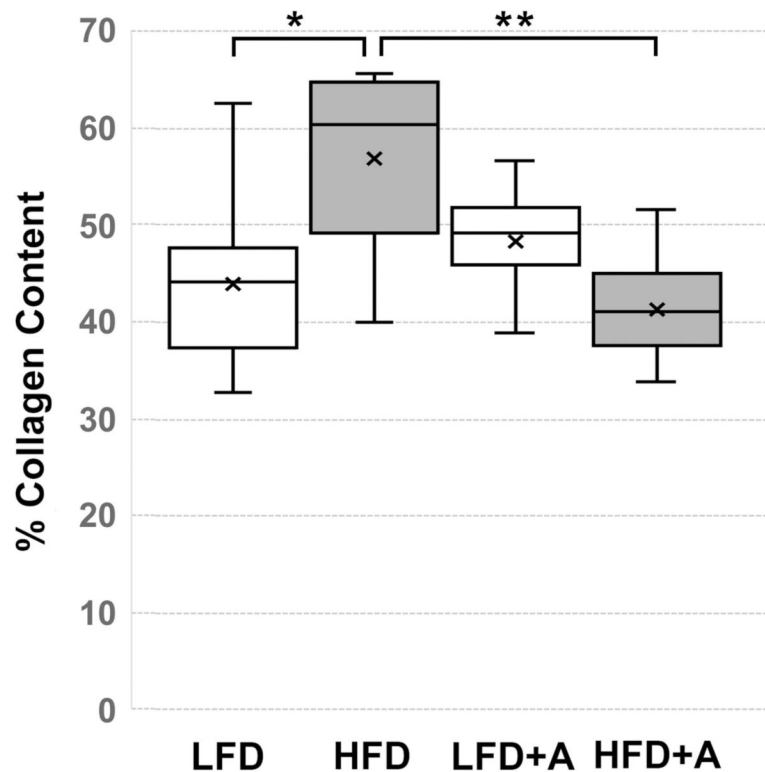
FIGURE 6.

Box and whisker plots of average collagen content of peri-urethral prostate tissues (as indicated in Figure 4) of HFD ($N = 11$), HFD + CXCR4 antagonist (HFD + A) ($N = 9$), LFD ($N = 7$), or LFD + CXCR4 antagonist (LFD + A) ($N = 12$) fed mice. The average collagen content of these tissues in HFD fed mice, 57(+/− 3.4)%, was significantly higher than that observed in LFD fed mice, 44 (+/− 2.7)% ($P < 0.01$). The average peri-urethral tissue collagen content of LFD + CXCR4 antagonist (LFD + A) fed mice, 48(+/− 2)%, was not significantly different from that of LFD fed mice. However, the average peri-urethral collagen content of HFD + A fed mice was significantly lower, 41(+/− 2)%, than that of HFD fed mice ($P < 0.001$). Box plots indicate lower extreme, lower quartile, median (line), mean (x), upper quartile and upper extreme. Statistical significance between groups is indicated as *, $P < 0.01$; **, $P < 0.001$; ***, $P > 0001$